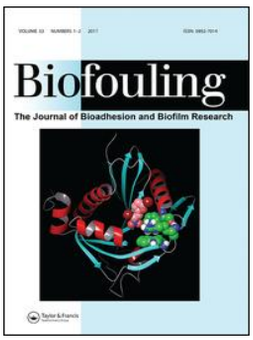

Biofouling

The Journal of Bioadhesion and Biofilm Research

ISSN: 0892-7014 (Print) 1029-2454 (Online) Journal homepage: https://www.tandfonline.com/loi/gbif20

# Structural changes in *S. epidermidis* biofilms after transmission between stainless steel surfaces

**Niar Gusnaniar, Jelmer Sjollema, Titik Nuryastuti, Brandon W. Peterson, Betsy van de Belt-Gritter, Ed D. de Jong, Henny C. van der Mei & Henk J. Busscher**

**To cite this article:** Niar Gusnaniar, Jelmer Sjollema, Titik Nuryastuti, Brandon W. Peterson, Betsy van de Belt-Gritter, Ed D. de Jong, Henny C. van der Mei & Henk J. Busscher (2017) Structural changes in *S. epidermidis* biofilms after transmission between stainless steel surfaces, Biofouling, 33:9, 712-721, DOI: 10.1080/08927014.2017.1360870

**To link to this article:** https://doi.org/10.1080/08927014.2017.1360870



Published online: 04 Sep 2017.

BIOFOULING, 2017
VOL. 33, NO. 9, 712–721
https://doi.org/10.1080/08927014.2017.1360870

Taylor & Francis
Taylor & Francis Group



# Structural changes in *S. epidermidis* biofilms after transmission between stainless steel surfaces

Niar Gusnaniar[a], Jelmer Sjollema[a], Titik Nuryastuti[b], Brandon W. Peterson[a], Betsy van de Belt-Gritter[a], Ed D. de Jong[a], Henny C. van der Mei[a] and Henk J. Busscher[a]

[a]Department of Biomedical Engineering, University of Groningen and University Medical Center Groningen, Groningen, the Netherlands; [b]Faculty of Medicine, Department of Microbiology, Universitas Gadjah Mada, Yogyakarta, Indonesia

**ABSTRACT**

Transmission is a main route for bacterial contamination, involving bacterial detachment from a donor and adhesion to receiver surfaces. This work aimed to compare transmission of an extracellular polymeric substance (EPS) producing and a non-EPS producing *Staphylococcus epidermidis* strain from biofilms on stainless steel. After transmission, donor surfaces remained fully covered with biofilm, indicating transmission through cohesive failure in the biofilm. Counter to the numbers of biofilm bacteria, the donor and receiver biofilm thicknesses did not add up to the pre-transmission donor biofilm thickness, suggesting more compact biofilms after transmission, especially for non-EPS producing staphylococci. Accordingly, staphylococcal density per unit biofilm volume had increased from 0.20 to 0.52 $\mu m^{-3}$ for transmission of the non-EPS producing strain under high contact pressure. The EPS producing strain had similar densities before and after transmission (0.17 $\mu m^{-3}$). This suggests three phases in biofilm transmission: (1) compression, (2) separation and (3) relaxation of biofilm structure to its pre-transmission density in EPS-rich biofilms.

**ARTICLE HISTORY**
Received 21 June 2017
Accepted 25 July 2017

**KEYWORDS**
*Staphylococcus epidermidis*; biofilm viscoelasticity; optical coherence tomography; CLSM; biofilm compaction; biofilm relaxation

## Introduction

Biofilms consist of bacteria adhering to the surface of a substratum, embedded in a matrix of extracellular polymeric substances (EPS) (Flemming and Wingender 2010; Hall-Stoodley et al. 2012). The structure of a biofilm can differ depending on the substratum surface and not only impacts the penetrability of the biofilm by nutrients (Nadell et al. 2009; Sjollema et al. 2011), but also by antimicrobials (Stewart and Costerton 2001; Donlan and Costerton 2002). Moreover, the viscoelasticity conveyed by the EPS matrix hampers detachment of biofilms by mechanical means (Stoodley et al. 2002; Flemming and Wingender 2010; Peterson et al. 2015). As a consequence, biofilms cause major problems in many different and widely varying environments, such as on biomaterial implants and devices (Hall-Stoodley and Stoodley 2005; Campoccia et al. 2013; Lebeaux et al. 2013), ships' hulls (Flemming 2002; Tribou and Swain 2015), water transport pipes (Juhna et al. 2007; Rhoads et al. 2016) and food packaging materials (Li et al. 2009; Nerín et al. 2016). Biofilm formation can be described by four distinct phases (Rendueles and Ghigo 2012): (1) transport from an aqueous suspension or air towards a substratum surface (Donlan and Costerton 2002; Nadell et al. 2009; Sjollema et al. 2011); (2) reversible adhesion to the substratum surface; (3) transition of an adhering organism from a planktonic to a sessile phenotype, producing EPS to cause irreversible adhesion; and (4) growth.

Although it is mostly assumed that transport occurs through convective-diffusion in an aqueous suspension or air, in many practical situations bacteria are transmitted from one surface to another under an applied contact pressure (Zapka et al. 2011). Transmission is an essentially different process from transport by convection or diffusion because it involves detachment of adhering bacteria from a donor surface followed by subsequent adhesion to a receiver surface (Van der Mei et al. 2010; Qu et al. 2011). Transmission is one of the main routes of bacterial contamination occurring in biomedical, domestic, environmental and industrial applications, either under compressive or shear loading of a biofilm-covered donor and an initially clean receiver surface. Bacterial transfer from urethral epithelial cells to urinary catheters for

**CONTACT** Henny C. van der Mei h.c.van.de.mei@umcg.nl

instance, occurs mainly under shear (Warren 2001; Siddiq and Darouiche 2012), while transmission between gloves from healthcare workers, the skin of a patient and hospital equipment occurs predominantly under compressive loading (Morgan et al. 2012). The epidemiological consequences of bacterial transmission between surfaces in hospital environments are amply studied and it is known that bacterially contaminated surfaces in hospital environments increase patients' risk of infection (Vickery et al. 2012; Cheng et al. 2015). Mechanisms of bacterial transmission, on the other hand, are seldom studied. Importantly, due to the involvement of a load during transmission, transmission may affect the structure and therewith the nutrient and antimicrobial penetrability of biofilms left-behind (Donlan and Costerton 2002; Nadell et al. 2009; Sjollema et al. 2011) on donor surfaces which are transmitted to receiver surfaces.

It was the aim of this study to compare biofilm transmission of *Staphylococcus epidermidis* ATCC 35984 (an EPS producing strain) and *S. epidermidis* 252 (a non-EPS producing strain) between two stainless steel surfaces under compression by applying two different contact pressures. Donor biofilm thicknesses before and after transmission as well as biofilm thicknesses on the receiver surfaces after transmission were determined using optical coherence tomography (OCT). Subsequently, the numbers of bacteria in donor and receiver biofilms were enumerated in a Bürker–Türk counting chamber after biofilm dispersal. In addition, biofilms were imaged using confocal laser scanning microscopy (CLSM) and two-photon-laser scanning microscopy (2P-LSM) (Neu et al. 2002). EPS production was inferred from the presence of calcofluor white stainable regions in fluorescent images of stained biofilms.

## Materials and methods

### Bacterial strains and growth condition

EPS producing *S. epidermidis* ATCC 35984 (Williams and Bloebaum 2010) and non-EPS producing *S. epidermidis* 252 were originally isolated from a patient with a catheter-associated sepsis and stool (Van der Mei et al. 1997), respectively. Both strains were grown aerobically for 24 h at 37°C on blood agar plates from frozen stocks. One single colony was used to make a pre-culture in 10 ml of tryptone soya broth (TSB, Oxoid, Basingstoke, UK) supplemented with 0.25% D(+)glucose, anhydrous ($C_6H_{12}O_6$, Merck, Darmstadt, Germany) and 0.5% NaCl (Merck), which was incubated for 24 h at 37°C. This 10 ml pre-culture was used to inoculate a second culture of 200 ml supplemented TSB, which was incubated for 16 h at 37°C and used for further experiments. The number of staphylococci in the culture suspension was $1 \times 10^9$ bacteria $ml^{-1}$, as measured using a Bürker–Türk counting chamber.

### Preparation of stainless steel surfaces and biofilm formation

Biofilm transmission was carried out between stainless steel 304 (SS) donor and receiver surfaces. SS plates with a surface area of 2.25 $cm^2$ (15 mm × 15 mm; 1 mm thickness) were cleaned by rinsing with 2% Extran® (Merck) followed by sonication for 5 min in 2% of RBS™35 (Sigma-Aldrich, St Louis, MO, USA) and rinsing with tap water, 70% ethanol and finally sterile, demineralised water. This yielded a water contact angle of 27 ± 4°.

In order to improve staphylococcal adhesion, the SS surfaces were first coated with serum proteins by immersion in 10% foetal bovine serum (FBS) (F7524, Sigma-Aldrich) in phosphate buffered saline (PBS) for 2 h under static conditions. After pipetting out the FBS solution, the FBS-coated stainless steel donor plates were placed on the bottom of Petri dishes filled with 15 ml of a staphylococcal suspension and left to allow bacterial adhesion for 1 h at 37°C. Next, the suspension was carefully removed after which the plates were placed into a Petri dish with 15 ml of fresh supplemented TSB medium. Subsequently, staphylococci were grown for 48 h at 37°C to form a biofilm. The medium was refreshed after 24 h.

For transmission and biofilm analysis, medium was pipetted carefully out of the Petri dishes and biofilm covered plates were placed into a new Petri dish with 10 ml of reduced transport fluid, pH 6.8 (RTF; NaCl 12 g $l^{-1}$, $(NH_4)_2SO_4$ 12 g $l^{-1}$, $KH_2PO_4$ 6 g $l^{-1}$, $Mg.SO_4.H_2O$ 2.5 g $l^{-1}$, $K_2HPO_4$ 6 g $l^{-1}$, $Na_2EDTA.2H_2O$ 41.2 g $l^{-1}$, L-cysteine. $HCl.H_2O$ 11.1 g $l^{-1}$) to enable transport of the biofilm covered plates to either of the instruments for biofilm characterisation.

### Biofilm transmission assay

First, for ease of handling, cork cylinders were glued to the backsides of the receiver plates. For transmission, RTF was pipetted out of the Petri dish and a SS receiver was pressed on top of the biofilm covered donor surface under a pressure of 0.7 or 7.0 kPa for 1 min. The pressures chosen are in the same range as the pressure of holding a cup of coffee or using a door handle, being around 2 kPa (Arinder et al. 2016). Next, donor and receiver surfaces were rapidly (<1 s) and perpendicularly separated from each other by keeping the donor plate in place with a pair of forceps and simultaneously lifting the receiver plate. Subsequently, both receiver and donor plates were immersed in RTF for further experiments. All experiments were carried out in triplicate with different staphylococcal cultures and samples. The numbers of staphylococci in the biofilm before and after transmission were determined by dispersal of the biofilms over the entire substratum area of 2.25 $cm^2$, using sterilised, 5 mm interdental brushes (Albert Heijn,

Zaandam, the Netherlands) in 5 ml of RTF while remaining in their Petri dishes. After brushing, the brush, plate and the RTF were put in a sterile tube and sonicated for 1 min to remove bacteria from the brush and plate and break bacterial aggregates. Subsequently, staphylococci were enumerated in a Bürker–Turk counting chamber. Staphylococcal transmission was expressed as a log-reduction of the number of bacteria on the donor plates according to:

$$^{10}\log\left(D_0 - R\right) - ^{10}\log\left(D_0\right)$$

in which $D_0$ is the number of staphylococci on the donor plate before transmission and $R$ the number of bacteria found on the receiver after transmission.

### OCT analysis of biofilms

The biofilms were analysed before transmission on the donor plates and after transmission on both donor and receiver plates with an OCT Ganymede II (Thorlabs Ganymade, Newton, NJ, USA), while keeping the plates immersed in the RTF. The biofilms were analysed on basis of 10 line scans on each donor and receiver plate by image post-processing of each line scan using Image J (National Institutes of Health, Bethesda, MD, USA), covering the entire substratum area of 2.25 $cm^2$. First, the bottom of the biofilm was determined as the best fitting line (second order polynomial) that connects the white pixels resulting from light reflection on the substratum surface. Subsequently a grey-value threshold that separates the biofilm from the background was calculated on basis of the grey-value histogram of the entire image (Otsu 1979). Then the upper contour line of the biofilm was defined as those pixels in the image that have a grey value just higher than the grey-value threshold and are connected to the bottom of the biofilm by pixels with grey values all higher than the grey-value threshold. The mean biofilm thickness per line scan was calculated based on the number of pixels between the bottom of the biofilm and the upper contour line. The overall biofilm thickness was defined as the average biofilm thickness over 10 line scans.

### Confocal laser scanning microscopy and two-photon laser microscopy

LIVE stain (*Bac*Light™, Molecular probes, Leiden, the Netherlands) containing SYTO9 (3.34 mM) was applied to the biofilms for 15 min in the dark at room temperature, followed by staining with fluorescent brightener 28 (50 mM) (Calcofluor white M2R; Sigma, St Louis, MO, USA) for 15 min to visualise EPS. It should be noted that calcofluor white only stains polysaccharides within an EPS matrix, as a main matrix component next to eDNA, proteins and possible other molecules. After staining, the biofilm was immersed in PBS and imaged using a CLSM (Leica TCS-SP2, Leica Microsystems Heidelberg GmbH, Heidelberg, Germany) at 40× magnification with laser excitation at 488 and 351 nm for SYTO9 and Fluorescent Brightener 28, respectively. Images were stacked and analysed using Fiji (Schindelin et al. 2012). The surface topography of the biofilms before and after transmission were analysed using two photon laser scanning microscopy (2P-LSM) after SYTO9 and fluorescent brightener 28 staining. Imaging was performed using a Zeiss LSM 7MP microscope (Zeiss, Jena, Germany) with Chameleon Vision compact OPO two photon laser (Coherent, Santa Clara, CA, USA). Excitation wavelengths of 825 nm were used and an emission filter set at 470–515 nm for SYTO9 or 435 nm for fluorescent brightener 28. Images were acquired and analysed using ZEN-lite imaging software (Carl Zeiss, Jena, Germany).

### Statistical analysis

The differences in biofilm properties before and after transmission were compared using two-tailed Student's *t*-test. Differences were considered significant if $p < 0.05$. Statistical analysis was performed using GraphPad Prism version 7.00 (GraphPad Software, La Jolla, CA, USA; www.graphpad.com).

## Results

### Staphylococcal biofilms on SS donor surfaces before transmission

Biofilms on SS surfaces fully covered the substratum surface and showed clear patches of calcofluor white stainable EPS in biofilms of *S. epidermidis* ATCC 35984, that were absent in biofilms of *S. epidermidis* 252 (Figure 1a). Topological imaging of the biofilms using 2P-LSM revealed mushroom-like structures in biofilms of EPS producing *S. epidermidis* ATCC 35984, while biofilms of the non-EPS producing strain were relatively smooth without mushroom-like structures (Figure 1b). This topological difference was confirmed in low-resolution, cross-sectional OCT images of biofilms (Figure 1c), showing a smaller thickness of 48 ± 9 µm for the EPS producing than for the non-EPS producing strain (70 ± 14 µm). Dispersal and subsequent microscopic enumeration of bacterial numbers in a biofilm indicated that *S. epidermidis* ATCC 35984 biofilms contained $7.4 \times 10^8$ bacteria adhering $cm^{-2}$ of substratum surface, while this number was twofold higher in biofilms of *S. epidermidis* 252 ($14 \times 10^8$ bacteria $cm^{-2}$). A combination of

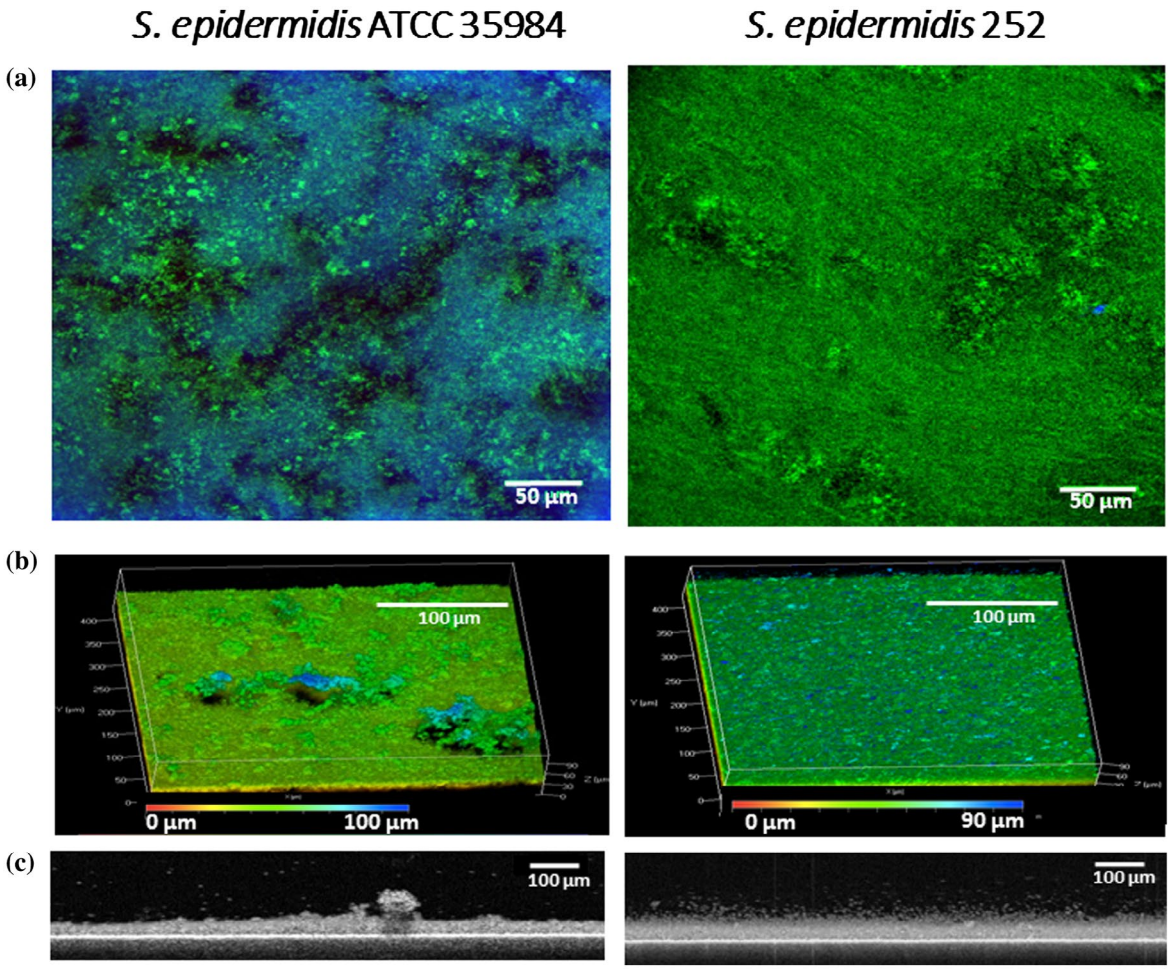


**Figure 1.** Structural features of EPS producing *S. epidermidis* ATCC 35984 and non-EPS producing *S. epidermidis* 252 biofilms on SS donor surfaces before transmission. (a) Projected top view CLSM overlayer images (green indicates bacteria, blue indicates the presence of EPS (ie calcofluor white stainable EPS components). (b) Surface topography from 2P-LSM (colours indicate the local height of the biofilm according to the pseudo-colour bars). (c) Cross-sectional OCT images (darker colours indicate water-rich regions).

**Table 1.** Summary of the structural features of biofilms on stainless steel donor surfaces before and after transmission.

| | EPS producing S. *epidermidis* ATCC 35984 | | | Non-EPS producing *S. epidermidis* 252 | | |
|---|---|---|---|---|---|---|
| | | After transmission | | | After transmission | |
| Method | Before transmission | 0.7 kPa | 7 kPa | Before transmission | 0.7 kPa | 7 kPa |
| CLSM | Full coverage with EPS patches | | | Full coverage without EPS | | |
| 2P-LSM | Mushroom-like structures | Elongated structures on top of biofilm surfaces | | Smooth biofilm surfaces | Smooth biofilm surfaces | |
| OCT | Mushroom-like structures | Full coverage without mushroom structures | | Smooth, but diffuse biofilm surface | Smooth, but slightly less diffuse biofilm surface | |
| Density (bacteria per µm$^3$) | 0.15 ± 0.07 | 0.20 ± 0.05 | 0.18 ± 0.13 | 0.20 ± 0.07* | 0.18 ± 0.08 | 0.52 ± 0.16* |

Transmitted biofilms on receiver surfaces were generally too thin for a comprehensive analysis of their features. Bacterial densities are averaged over three separately grown biofilms out of different cultures with ± indicating SDs Asterisks indicate significant differences between densities before and after transmission.

these bacterial numbers per unit area with the thicknesses measured in OCT provided bacterial densities per unit biofilm volume, which were slightly lower before transmission in biofilms of the EPS producing staphylococcus (0.15 µm$^{-3}$) than of the non-EPS producing staphylococcus (0.20 µm$^{-3}$). In addition, the OCT images of *S. epidermidis* ATCC 35984 biofilms possessed a more granular structure, with small black regions indicative of water-filled regions (Wagner et al. 2010; Blauert et al. 2015), opposite to more homogeneously grey-looking biofilms of non-EPS producing *S. epidermidis* 252.

Table 1 summarises the qualitative and quantitative features of both staphylococcal biofilms before transmission.

### *Staphylococcal biofilms on SS donor surfaces after transmission*

OCT images (Figure 2a and b) clearly show that the donor surfaces after transmission remained fully covered with biofilm, while the receiver surfaces show patchy coverage after transmission of *S. epidermidis* ATCC 35984 and only a very thin film after *S. epidermidis* 252 transmission. Donor biofilms of EPS producing *S. epidermidis* ATCC 35984 were flattened during transmission, and mushroom-like structures, as observed on donor biofilms before transmission, had disappeared. OCT images for both staphylococcal strains looked more homogeneously grey and sharper confined than before transmission (compare Figure 1c with Figure 2a and b). After transmission of EPS-producing *S. epidermidis* ATCC 35984, elongated structures could be seen in 2P-LSM micrographs on the

**Table 2.** Sequential phases in biofilm transmission between two surfaces and associated structural changes in the presence and absence and of an EPS matrix, as concluded from observations on an EPS producing and a non-EPS producing *S. epidermidis* strain.

| Phase | EPS producing *S. epidermidis* ATCC 35984 | | Non-EPS producing *S. epidermidis* 252 | |
|---|---|---|---|---|
| (1) Compression | • Bacteria are forced closer together yielding a compact biofilm<br>• Water with soluble EPS components is squeezed out of the biofilm | | • Bacteria are forced closer together yielding a compact biofilm<br>• Water is squeezed out of the biofilm | |
| (2) Separation | Donor<br>• Bacteria are forced apart from each other<br>• Cohesive failure in the biofilm<br>• Formation of EPS threads during failure<br>• Collapse of EPS threads on biofilm left on donor surface | Receiver<br>• Patch-wise, low coverage | Donor<br>• Bacteria are forced apart from each other<br>• Cohesive failure in the biofilm | Receiver<br>• High coverage of biofilm with low biofilm density |
| (3) Relaxation | • Viscoelastic relaxation further restores water-filled regions and reduces bacterial density in the biofilm | | • Absence of viscoelastic relaxation leaves a biofilm with a high bacterial density | |

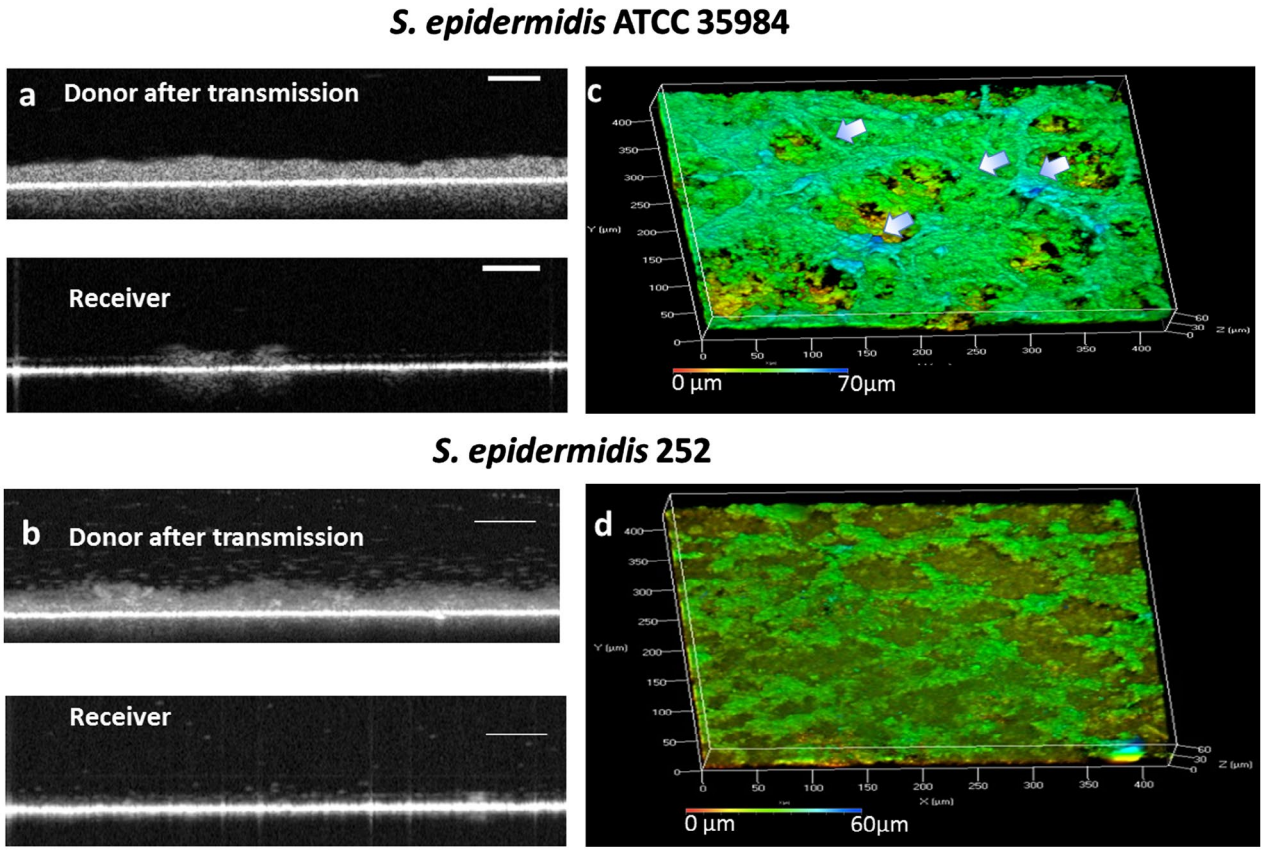


**Figure 2.** Examples of cross-sectional OCT images of staphylococcal biofilms of EPS producing *S. epidermidis* ATCC 35984 (a), and (b) non-EPS producing *S. epidermidis* 252 on SS donor and receiver surfaces after transmission at an applied pressure of 0.7 kPa for 1 min. Scale bars = 100 µm. (c, d) Surface topography from 2P-LSM (colours indicate the local height of the biofilm as indicated by the pseudo-colour bars) of biofilms on the SS donor surfaces after transmission for EPS producing *S. epidermidis* ATCC 35984 (c) and (d) non-EPS producing *S. epidermidis* 252 (right panel) at a pressure of 0.7 kPa. Arrows indicate elongated structures.

surface of donor biofilms that were absent in donor biofilms after transmission of the non-EPS producing strain (compare Figure 2c and d).

Biofilm thicknesses on receiver surfaces were significantly thinner than of biofilms remaining on the donor surfaces (Figure 3), regardless of the contact pressure applied. Receiver biofilms of EPS producing *S. epidermidis* ATCC 35984 (Figure 3a) were significantly thinner than of non-EPS producing *S. epidermidis* 252 (Figure 3b). Interestingly, the total thickness after transmission on donor and receiver surfaces did not add up to the biofilm thickness on the donor before transmission, suggesting either loss of biofilm during the transmission process or structural changes induced during transmission. Significant loss of bacteria from the biofilms during transmission can be ruled out however, because the numbers of bacteria on donor and receiver surfaces after transmission did add up to the numbers of bacteria counted on donor surfaces before transmission (Figure 3c and d).

A combination of biofilm thicknesses and numbers of bacteria in biofilms per unit area on donor surfaces after transmission shows (see Table 1) that after transmission,

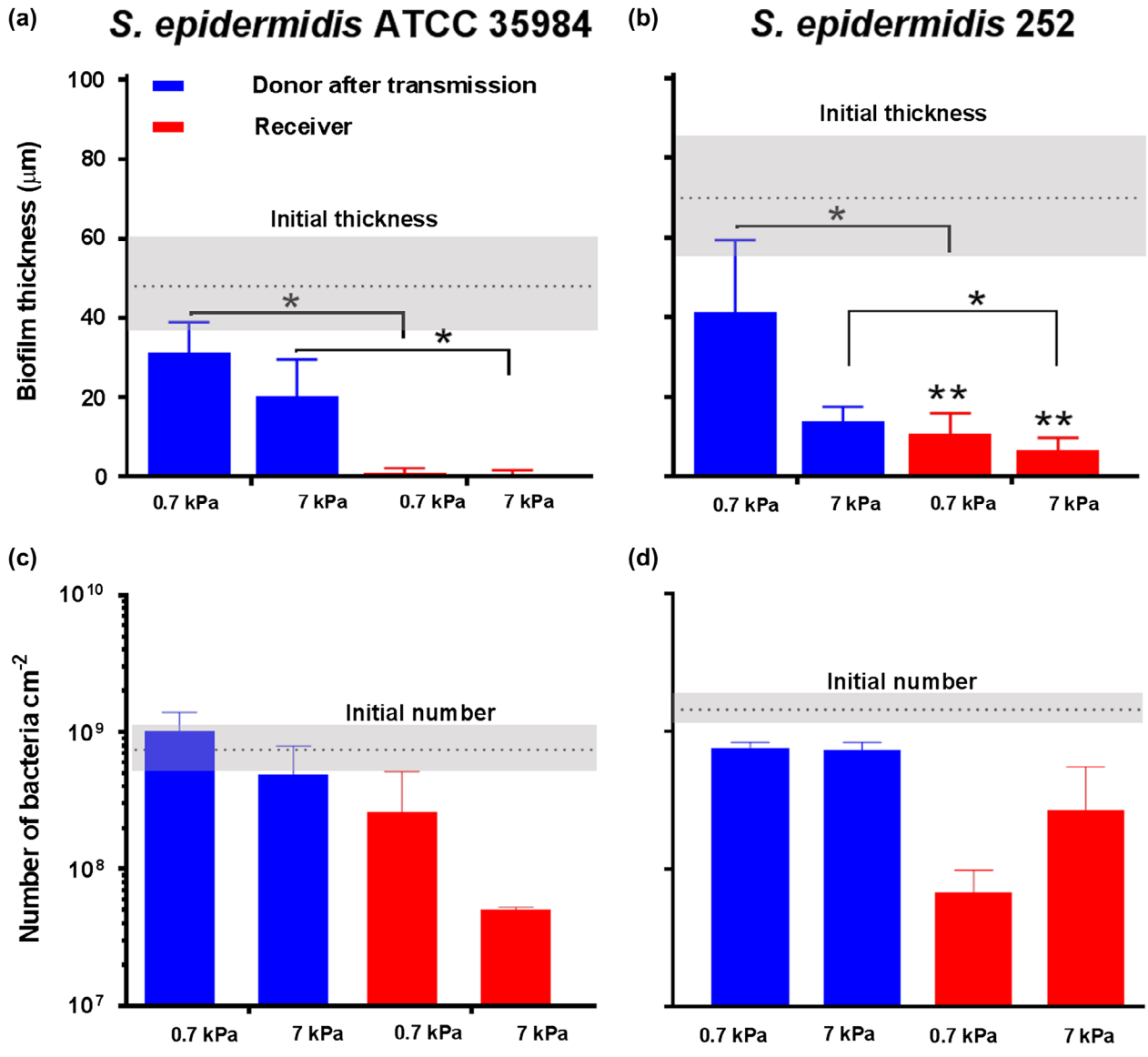


**Figure 3.** Staphylococcal biofilm thickness and numbers of bacteria in biofilms on SS donor and receiver surfaces after transmission at two different pressures applied after a contact time of 1 min. (a) thickness of EPS producing *S. epidermidis* ATCC 35984 biofilms; (b) the same as panel (a), for non-EPS producing *S. epidermidis* 252; (c) number of bacteria in *S. epidermidis* ATCC 35984 biofilms; (d) the same as panel (c), for *S. epidermidis* 252. Dotted lines with dashed regions represent the thickness of and numbers of staphylococci in biofilms on the donor surface before transmission with their SDs, while error bars indicate the SDs over three measurements with three separate bacterial cultures. Asterisks indicate significant differences between biofilm thicknesses on donor substrata and thicknesses on receiver surfaces. Double asterisks indicate significant differences between biofilm thicknesses on receiver surfaces of *S. epidermidis* ATCC 35984 and of *S. epidermidis* 252.

the biofilm densities per unit volume of *S. epidermidis* ATCC 35984 on the donor surfaces were similar (0.15–0.20 $\mu m^{-3}$) before and after transmission (biofilms on receiver surfaces were too thin and heterogeneously distributed for these kind of calculations). However, after transmission under the high pressure, bacterial densities in biofilms of the non-EPS producing *S. epidermidis* 252 increased significantly from 0.20 to 0.52 $\mu m^{-3}$.

## Discussion

Transmission is a common pathway for bacterial contamination of surfaces in diverse environments. In this paper, the structure of staphylococcal biofilms between a SS donor and a receiver surface before and after transmission were compared. Regardless of EPS production, ie calcofluor white stainable matrix components, donor surfaces remained fully covered with biofilm after transmission, which indicates that transmission occurred through cohesive failure in the biofilm since donor biofilms left behind were thinner than before transmission. EPS played a crucial role in restoring the structure of biofilms after transmission, which is proposed to be regarded as a three-phase process, involving: (1) compression of the biofilm under the applied contact pressure, (2) separation exerting a tensile stress on biofilm inhabitants and (3) relaxation (Table 2). Each of these three phases will be discussed in the next subsections.

### *Compression*

The first step in bacterial transmission between surfaces is compression of the biofilm between the donor and receiver surfaces by an external contact pressure. Water along with dissolved EPS components will be squeezed out first, as it has the lowest viscosity (Peterson et al. 2013). Also, bacteria will redistribute themselves slowly to new, energetically favourable positions. As a net result, bacteria will come closer together and the biofilm will become more compact. Evidence for compaction during the compression phase is indirect, as biofilms cannot be imaged or analysed when compressed between two plates. However, the higher bacterial densities in biofilms of the non-EPS producing strain after transmission under a contact pressure of 7 kPa can only have arisen during this compaction phase. Compression under a contact pressure 0.7 kPa for 1 min may be too small to yield compaction. Stress–strain diagrams for oral streptococci have a linear elastic trajectory for strains < 0.4, corresponding roughly with a stress of 0.1 kPa, which is in the same range as 0.7 kPa (Paramonova et al. 2009). Partly irreversible compaction up to 50%, however, was observed in biofilms generated in a cross-flow filtration model system by applying a transmembrane pressure in the order of 40–100 kPa (Dreszer et al. 2014). These findings confirm that a critical difference in biofilm response is realistic to expect between contact pressure of 0.7 and 7 kPa, as seen in this paper.

### *Separation*

Separation subjects the compacted biofilms to a tensile pressure, ultimately leading to detachment. Detachment occurs relatively rapidly and can either result from failure at the donor–biofilm interface or cohesive failure within the biofilm. Since, after transmission, donor surfaces remain fully covered by biofilm regardless of the strain involved, this indicates that biofilm is transmitted through cohesive failure within the biofilm and subsequent attachment of detached biofilm to the receiver surface. The separation phase is also difficult to visualise in between two plates. However, the presence of collapsed EPS threads on the surface of biofilms of the EPS producing staphylococcal strain, and their absence on biofilms of the non-EPS producing strain, suggest their formation during separation. In contrast to solids under tensile strength, where fracture occurs after the yield point, viscoelastic materials show necking or thinning, which may be the origin of the collapsed threads observed after separation for the EPS-producing strain (Alpkvist et al. 2006). Dunsmore et al. (2002) described a very similar yet distinctly different process for biofilms grown under high and low flow, showing formation of so-called 'streamlined' biofilm clusters under high flow.

### *Relaxation*

All biofilms, but especially EPS containing biofilms, relax after application of stress, regardless of whether compressive or tensile (Stoodley et al. 1999; Guélon et al. 2011; Peterson et al. 2015), to restore biofilm structure as much as possible. Usually, different components of a biofilm relax with their own characteristic time constants. After transmission as studied here, full restoration of biofilm structure has not been observed depending on the strain considered. In biofilms with more viscous components, relaxation occurs more swiftly (Alpkvist et al. 2006) than in the case of more rigid biofilms (Peterson et al. 2013) and accordingly the more viscous, EPS producing staphylococcal strain used in this study recovered its bacterial density to a higher degree than the more rigid biofilms of the non-EPS producing strain. The non-EPS producing strain demonstrated lasting structural changes that were most evident from the doubling of the bacterial density in *S. epidermidis* 252 donor biofilms after transmission under high contact pressure (7 kPa). The EPS matrix in *S. epidermidis* ATCC 35984 biofilms, on the other hand, facilitated recovery of the bacterial density to pre-transmission values.

The arguments above rely in part on the calculation of bacterial densities in the biofilms. Such calculations have been made possible through the use of OCT, enabling reliable determination of biofilm thickness over much larger areas than can be done with microscopic techniques, usually comprising a field of view of only several hundreds of square micrometres. In OCT, biofilm thickness can be obtained over several square centimetres. In combination with the number of bacteria in a biofilm per unit substratum area, thickness then yields the volumetric bacterial density in a biofilm. Bacterial densities in a biofilm have not been frequently reported in the literature, although they are very helpful for extracting structural data from them in a simple but unequivocal way. Distances between individual bacteria in a biofilm range between 1 and 3 μm (Drescher et al. 2016). Microbial volume fractions in biofilm models have been calculated to range from 0.1 to 0.2, corresponding with bacterial densities between 0.2 and 0.4 $\mu m^{-3}$ (Wanner and Reichert 1996; Roberts and Stewart 2004). Experimentally obtained dry weights of ~60 mg $cm^{-3}$ of 50 to 100 μm thickness biofilms (Bishop et al. 1995) combined with published bacterial mass densities (Loferer-Krössbacher et al. 1998) yielded a bacterial density of around 0.3 $\mu m^{-3}$. These data show that the bacterial densities obtained using OCT thicknesses and bacterial numbers after biofilm dispersal are all realistic, both before and after transmission. Importantly, after transmission of the non-EPS producing strain, bacterial densities remained well below the closest hexagonal packing of a 1 μm diameter sphere for which a bacterial density of 1.5 $\mu m^{-3}$ can be calculated. From this, it can be concluded that staphylococci are not yet compressed to their maximum density under a contact pressure of 7 kPa. Whereas non-EPS producing *S. epidermidis* 252 was unable to recover from this compaction due to the lack of a visco-elastic matrix, *S. epidermidis* ATCC 35984 recovered to its pre-transmission density of around 0.18 $\mu m^{-3}$.

In conclusion, this paper introduced a three-phase biofilm transmission model, in which EPS plays a crucial role in defining the structure of biofilms after transmission. Transmission occurs through cohesive failure in the biofilms and after transmission, compacted biofilms can relax from the compression phase to their pre-transmission structure utilising the viscoelasticity of their EPS matrix.

## Acknowledgements

The authors would like to thank Dr Edward Rochford for his assistance with two-photon-laser microscopy.

## Disclosure statement

This publication reflects the views only of the authors, and the European Commission cannot be held responsible for any use which may be made of the information contained therein. HJB is also director of a consulting company SASA BV. Opinions and assertions contained herein are those of the authors and are not construed as necessarily representing the views of the funding organization or their respective employer(s).

## Funding

This research was funded with support from the European Commission through a LOTUS III Erasmus grant.

## References

Alpkvist E, Picioreanu C, Van Loosdrecht MCM, Heyden A. 2006. Three-dimensional biofilm model with individual cells and continuum EPS matrix. Biotechnol Bioeng. 94:961–979. doi: 10.1002/(ISSN)1097-0290

Arinder P, Johannesson P, Karlsson I, Borch E. 2016. Transfer and decontamination of *S. aureus* in transmission routes regarding hands and contact surfaces. PLoS ONE. 11:e0156390. doi: 10.1371/journal.pone.0156390

Bishop P, Zhang T, Fu Y. 1995. Effects of biofilm structure, microbial distributions and mass transport on biodegradation processes. Water Sci Technol. 31:143–152. doi: 10.1016/0273-1223(95)00162-G

Blauert F, Horn H, Wagner M. 2015. Time-resolved biofilm deformation measurements using optical coherence tomography. Biotechnol Bioeng. 112:1893–1905. doi: 10.1002/bit.25590

Campoccia D, Montanaro L, Arciola CR. 2013. A review of the clinical implications of anti-infective biomaterials and infection-resistant surfaces. Biomaterials. 34:8018–8029. doi: 10.1016/j.biomaterials.2013.07.048

Cheng VCC, Chau PH, Lee WM, Ho SKY, Lee DWY, So SYC, Wong SCY, Tai JWM, Yuen KY. 2015. Hand-touch contact assessment of high-touch and mutual-touch surfaces among healthcare workers, patients, and visitors. J Hosp Infect. 90:220–225. doi: 10.1016/j.jhin.2014.12.024

Donlan RM, Costerton JW. 2002. Biofilms: survival mechanisms of clinically relevant microorganisms. Clin Microbiol Rev. 15:167–193. doi: 10.1128/CMR.15.2.167-193.2002

Drescher K, Dunkel J, Nadell CD, Van Teeffelen S, Grnja I, Wingreen NS, Stone HA, Bassler BL. 2016. Architectural transitions in *Vibrio cholerae* biofilms at single-cell resolution. Proc Natl Acad Sci. 113:E2066–E2072. doi: 10.1073/pnas.1601702113

Dreszer C, Wexler AD, Drusová S, Overdijk T, Zwijnenburg A, Flemming H-C, Kruithof JC, Vrouwenvelder JS. 2014. In-situ biofilm characterization in membrane systems using optical coherence tomography: formation, structure, detachment and impact of flux change. Water Res. 67:243–254. doi: 10.1016/j.watres.2014.09.006

Dunsmore BC, Jacobsen A, Hall-Stoodley L, Bass CJ, Lappin-Scott HM, Stoodley P. 2002. The influence of fluid shear on the structure and material properties of sulphate-reducing bacterial biofilms. J Ind Microbiol Biotechnol. 29:347–353. doi: 10.1038/sj.jim.7000302

Flemming H-C. 2002. Biofouling in water systems – cases, causes and countermeasures. Appl Microbiol Biotechnol. 59:629–640. doi: 10.1007/s00253-002-1066-9

Flemming H-C, Wingender J. 2010. The biofilm matrix. Nat Rev Microbiol. 8:623–633.

Guélon T, Mathias J-D, Stoodley P. 2011. Advances in biofilm mechanics. In: Flemming H-C, Wingender J, Szewzyk U, editors. Biofilm highlights. Berlin Heidelberg, Berlin, Heidelberg: Springer; p. 111–139. doi: 10.1007/978-3-642-19940-0

Hall-Stoodley L, Stoodley P. 2005. Biofilm formation and dispersal and the transmission of human pathogens. Trends Microbiol. 13:7–10. doi: 10.1016/j.tim.2004.11.004

Hall-Stoodley L, Stoodley P, Kathju S, Høiby N, Moser C, William Costerton J, Moter A, Bjarnsholt T. 2012. Towards diagnostic guidelines for biofilm-associated infections. FEMS Immunol Med Microbiol. 65:127–145. doi: 10.1111/j.1574-695X.2012.00968.x

Juhna T, Birzniece D, Larsson S, Zulenkovs D, Sharipo A, Azevedo NF, Menard-Szczebara F, Castagnet S, Feliers C, Keevil CW. 2007. Detection of *Escherichia coli* in biofilms from pipe samples and coupons in drinking water distribution networks. Appl Environ Microbiol. 73:7456–7464. doi: 10.1128/AEM.00845-07

Lebeaux D, Chauhan A, Rendueles O, Beloin C. 2013. From *in vitro* to *in vivo* models of bacterial biofilm-related infections. Pathogens. 2:288–356. doi: 10.3390/pathogens2020288

Li X, Xing Y, Jiang Y, Ding Y, Li W. 2009. Antimicrobial activities of ZnO powder-coated PVC film to inactivate food pathogens. Int J Food Sci Technol. 44:2161–2168. doi: 10.1111/ifs.2009.44.issue-11

Loferer-Krössbacher M, Klima J, Psenner R. 1998. Determination of bacterial cell dry mass by transmission electron microscopy and densitometric image analysis. Appl Environ Microbiol. 64:688–694.

Morgan DJ, Rogawski E, Thom KA, Johnson JK, Perencevich EN, Shardell M, Leekha S, Harris AD. 2012. Transfer of multidrug-resistant bacteria to healthcare workers' gloves and gowns after patient contact increases with environmental contamination. Crit Care Med. 40:1045–1051. doi: 10.1097/CCM.0b013e31823bc7c8

Nadell CD, Xavier JB, Foster KR. 2009. The sociobiology of biofilms. FEMS Microbiol Rev. 33:206–224. doi: 10.1111/j.1574-6976.2008.00150.x

Nerín C, Aznar M, Carrizo D. 2016. Food contamination during food process. Trends Food Sci Technol. 48:63–68. doi: 10.1016/j.tifs.2015.12.004

Neu TR, Kuhlicke U, Lawrence JR. 2002. Assessment of fluorochromes for two-photon laser scanning microscopy of biofilms. Appl Environ Microbiol. 68:901–909. doi: 10.1128/AEM.68.2.901-909.2002

Otsu N. 1979. A threshold selection method from gray-level histograms. IEEE Trans Syst Man Cybern. 9:62–66. doi: 10.1109/TSMC.1979.4310076

Paramonova E, Kalmykowa OJ, Van der Mei HC, Busscher HJ, Sharma PK. 2009. Impact of hydrodynamics on oral biofilm strength. J Dent Res. 88:922–926. doi: 10.1177/0022034509344569

Peterson BW, Van der Mei HC, Sjollema J, Busscher HJ, Sharma PK. 2013. A distinguishable role of eDNA in the viscoelastic relaxation of biofilms. MBio. 4:e00497.

Peterson BW, He Y, Ren Y, Zerdoum A, Libera MR, Sharma PK, Van Winkelhoff AJ, Neut D, Stoodley P, Van der Mei HC, Busscher HJ. 2015. Viscoelasticity of biofilms and their recalcitrance to mechanical and chemical challenges. FEMS Microbiol Rev. 39:234–245. doi: 10.1093/femsre/fuu008

Qu W, Busscher HJ, Hooymans JMM, Van der Mei HC. 2011. Surface thermodynamics and adhesion forces governing bacterial transmission in contact lens related microbial keratitis. J Colloid Interface Sci. 358:430–436. doi: 10.1016/j.jcis.2011.03.062

Rendueles O, Ghigo J-M. 2012. Multi-species biofilms: how to avoid unfriendly neighbors. FEMS Microbiol Rev. 36:972–989. doi: 10.1111/j.1574-6976.2012.00328.x

Rhoads W, Pruden A, Edwards M. 2016. Convective mixing in distal pipes exacerbates *Legionella pneumophila* growth in hot water plumbing. Pathogens. 5:29. doi: 10.3390/pathogens5010029

Roberts ME, Stewart PS. 2004. Modeling antibiotic tolerance in biofilms by accounting for nutrient limitation. Antimicrob Agents Chemother. 48:48–52. doi: 10.1128/AAC.48.1.48-52.2004

Schindelin J, Arganda-Carreras I, Frise E, Kaynig V, Longair M, Pietzsch T, Preibisch S, Rueden C, Saalfeld S, Schmid B, et al. 2012. Fiji: an open-source platform for biological-image analysis. Nat Methods. 9:676–682. doi: 10.1038/nmeth.2019

Siddiq DM, Darouiche RO. 2012. New strategies to prevent catheter-associated urinary tract infections. Nat Rev Urol. 9:305–314. doi: 10.1038/nrurol.2012.68

Sjollema J, Rustema-Abbing M, Van der Mei HC, Busscher HJ. 2011. Generalized relationship between numbers of bacteria and their viability in biofilms. Appl Environ Microbiol. 77:5027–5029. doi: 10.1128/AEM.00178-11

Stewart PS, Costerton JW. 2001. Antibiotic resistance of bacteria in biofilms. Lancet. 358:135–138. doi: 10.1016/S0140-6736(01)05321-1

Stoodley P, Lewandowski Z, Boyle JD, Lappin-Scott HM. 1999. Structural deformation of bacterial biofilms caused by short-term fluctuations in fluid shear: an *in situ* investigation of biofilm rheology. Biotechnol Bioeng. 65:83–92. doi: 10.1002/(ISSN)1097-0290

Stoodley P, Cargo R, Rupp CJ, Wilson S, Klapper I. 2002. Biofilm material properties as related to shear-induced deformation and detachment phenomena. J Ind Microbiol Biotechnol. 29:361–367. doi: 10.1038/sj.jim.7000282

Tribou M, Swain GW. 2015. Grooming using rotating brushes as a proactive method to control ship hull fouling. Biofouling. 31:309–319. doi: 10.1080/08927014.2015.1041021

Van der Mei HC, De Vries J, Busscher HJ. 2010. Weibull analyses of bacterial interaction forces measured using AFM. Colloids Surf B Biointerfaces. 78:372–375. doi: 10.1016/j.colsurfb.2010.03.018

Van der Mei HC, Van de Belt-Gritter B, Reid G, Bialkowska-Hobrzanska H, Busscher HJ. 1997. Adhesion of coagulase-negative staphylococci grouped according to physico-chemicaI surface properties. Microbiology. 143:3861–3870. doi: 10.1099/00221287-143-12-3861

Vickery K, Deva A, Jacombs A, Allan J, Valente P, Gosbell IB. 2012. Presence of biofilm containing viable multiresistant organisms despite terminal cleaning on clinical surfaces in an intensive care unit. J Hosp Infect. 80:52–55. doi: 10.1016/j.jhin.2011.07.007

Wagner M, Taherzadeh D, Haisch C, Horn H. 2010. Investigation of the mesoscale structure and volumetric features of biofilms using optical coherence tomography. Biotechnol Bioeng. 107:844–853. doi: 10.1002/bit.22864

Wanner O, Reichert P. 1996. Mathematical modeling of mixed-culture biofilms. Biotechnol Bioeng. 49:172–184. doi: 10.1002/(ISSN)1097-0290

Warren JW. 2001. Catheter-associated urinary tract infections. Int J Antimicrob Agents. 17:299–303. doi: 10.1016/S0924-8579(00)00359-9

Williams DL, Bloebaum RD. 2010. Observing the biofilm matrix of *Staphylococcus epidermidis* ATCC 35984 grown using the CDC biofilm reactor. Microsc Microanal. 16:143–152. doi: 10.1017/S143192760999136X

Zapka CA, Campbell EJ, Maxwell SL, Gerba CP, Dolan MJ, Arbogast JW, Macinga DR. 2011. Bacterial hand contamination and transfer after use of contaminated bulk-soap-refillable dispensers. Appl Environ Microbiol. 77:2898–2904. doi: 10.1128/AEM.02632-10